PHYSICAL REVIEW

LETTERS

VOLUME 61 | 18 JULY 1988 | NUMBER 3

Quantum Billiard in a Magnetic Field: Chaos and Diamagnetism

K. Nakamura[a]

Department of Physics, Fukuoka Institute of Technology, Higashi-ku, Fukuoka 811-02, Japan

and

H. Thomas

Institut für Physik der Universität Basel, CH-4056 Basel, Switzerland

(Received 27 January 1988)

The quantum mechanics of noninteracting electrons is studied in a nonintegrable elliptic billiard with a uniform magnetic field applied perpendicularly. We make an attempt to establish a connection between chaotic dynamics and macroscopic quantum observables. For small two-dimensional systems, a remarkable reduction and large fluctuations of the diamagnetic susceptibility are found in the corresponding classically chaotic region.

PACS numbers: 05.45.+b, 03.65.−w, 75.20.−g

Despite the accumulation of studies on complicated energy spectra of quantum chaos, most of the activity has rather concentrated on local aspects of the spectra, i.e., on level-spacing distribution and spectral rigidity at fixed values of nonintegrability parameters.[1] But global aspects, e.g., sensitivity of energies to the change of these parameters, await much more profound investigations.[2] On the other hand, the spirit of natural science requires us to find realizations of quantum chaos, and thereby to establish the connection between chaotic dynamics and experimentally accessible macroscopic quantum observables.

In this Letter, we consider the quantum mechanics of noninteracting electrons in a planar billiard (e.g., a thin conducting disk) in a uniform magnetic field normal to the plane. The shape of the boundary is taken as elliptic. Unless the boundary effects are taken into consideration, quantum-mechanical treatment merely yields the Landau diamagnetic susceptibility.[3] (As for the puzzle of the vanishing susceptibility in classical statistical mechanics, see the review by Peierls.[4]) Recent analysis of single-electron classical dynamics,[5] however, elucidated the onset of chaos in the case where the cyclotron radius is comparable to the linear dimension of the billiard, indicating the crucial role of the convex boundary. Quantum aspects of chaos will be captured by the incorporation of Dirichlet-type boundary conditions. In the following, we shall first solve the Dirichlet eigenvalue problem for a single-electron system. Then, global aspects of the spectra, i.e., the sensitivities of energies and their average over "occupied" levels—the diamagnetic susceptibility at absolute zero—will be investigated by our changing the magnetic field. Effects of lattice discreteness and of spin degrees of freedom will be suppressed in the present treatment.

Let us consider an ellipse with area $\pi L^2=\pi ab$ where a and b are semimajor and semiminor axes, in the x and y directions, respectively. The eigenvalue problem is given by $H\Psi=E\Psi$ with $\Psi=0$ at the boundary. Here $H=(1/2m)[(\hbar/i)\nabla+(e/c)\mathbf{A}]^2$. We take a symmetric gauge: $\mathbf{A}=(-\frac{1}{2}yB,\frac{1}{2}xB)$ with B the magnetic field. The present system has C_2 (inversion) symmetry. Let us consider the map $(x,y)\rightarrow(r,\theta)$ via $x=ar\cos\theta$, $y=br\sin\theta$. Then, the eigenvalue problem is reduced to $\tilde{H}(r,\theta)\tilde{\Psi}(r,\theta)=E\tilde{\Psi}(r,\theta)$ with $\tilde{\Psi}=0$ at the boundary of the unit disk. Basis functions are now constructed in terms of integer-order Bessel functions as $\{|kn\rangle\}\equiv\{R_{kn}J_k(\gamma_{kn}r)e^{ik\theta}\}$, where γ_{kn} are zeros of $J_k(z)$ and $R_{kn}\equiv[\sqrt{\pi}J_{k+1}(\gamma_{kn})]^{-1}$ are normalization constants. The $\{|kn\rangle\}$ are arranged in order of increasing values of

γ_{kn}^2. Nonvanishing matrix elements of $\tilde{H}$ are given in dimensionless form as

$$(\hbar^2/2mL^2)^{-1}\langle k'n'|\tilde{H}|kn\rangle=(\pi/2)(1+\sigma^2)\{[2\gamma_{kn}^2/(\bar{a}\sigma)^2+2\bar{B}k/\sigma]\Gamma_{kn'kn}^{(1)}+(\bar{B}^2\bar{a}^2/2)\Gamma_{kn'kn}^{(3)}\}$$

for $k'=k$ and

$$(\pi/2)(1-\sigma^{-2})\{-2[(k+1)/\bar{a}^2]\gamma_{kn}\Lambda_{k'n'kn}^{(0)}+(\gamma_{kn}^2/\bar{a}^2)\Gamma_{k'n'kn}^{(1)}+(\bar{B}\gamma_{kn}/\sigma)\Lambda_{k'n'kn}^{(2)}+(\bar{B}^2\bar{a}^2/4)\Gamma_{k'n'kn}^{(3)}\}$$

for $k'=k+2$ together with their real symmetric counterparts ($k'\leftrightarrow k, n'\leftrightarrow n$). Here

$$\Gamma_{k'n'kn}^{(l)}\equiv R_{k'n'}R_{kn}\int_0^1 r^l J_{k'}(\gamma_{k'n'}r)J_k(\gamma_{kn}r)dr$$

and $\Lambda_{k'n'kn}^{(l)}$ is given by the replacement of the last factor in this integrand by $J_{k+1}(\gamma_{kn}r)$. Further, we have introduced the dimensionless parameters $\sigma=b/a$, $\bar{a}=a/L$, $\bar{b}=b/L$, and $\bar{B}=B(c\hbar/eL^2)^{-1}$. From these matrix elements, we recognize the following: (i) The Hilbert space is decomposed into two subspaces of even ($k=0, \pm 2,\ldots$) and odd ($k=\pm 1,\pm 3,\ldots$) parity; (ii) in the case of $\sigma=1$, k is a good quantum number (i.e., angular momentum); (iii) for $\bar{B}=0$ with $\sigma=1$, eigenvalues reduce to $E=(\hbar^2/2mL^2)\gamma_{kn}^2$. In each of the two subspaces, we have taken the lowest 150 basis functions and computed the integrals $\Gamma_{k'n'kn}^{(l)}$, $\Lambda_{k'n'kn}^{(l)}$, and thereby $\langle k'n'|\tilde{H}|kn\rangle$. Then, we have solved the eigenvalue problem for the dimensionless matrix above separately in each manifold, to obtain scaled energies $\bar{E}=E(\hbar^2/2mL^2)^{-1}$, in the range $0<\sigma\leqq 1$ and $0\leqq\bar{B}\leqq 50$. In our changing σ, the area of the billiard has been kept constant: $\bar{a}=1/\sqrt{\sigma}$, $\bar{b}=\sqrt{\sigma}$. We have checked the reliability of decimal places of the eigenvalues by comparing them with the corresponding values obtained from enlarged (200×200) matrices. We find that about the lowest 50 eigenvalues for each parity have sufficient precision for our study. Below we present the results for a nonintegrable case, $\sigma=0.5$ (elliptic billiard), and the integrable case $\sigma=1$ (circular billiard). Comparison of the two cases helps to elucidate the effects of nonintegrability.

In Fig. 1, the even-parity part of the energy spectra is shown. In both Figs. 1(a) and 1(b), most of the levels

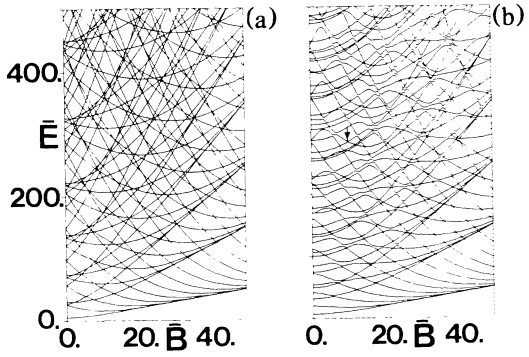

FIG. 1. $\bar{B}$-dependent energy spectra for the even-parity manifold: (a) circle billiard ($\sigma=1$); (b) ellipse billiard ($\sigma=0.5$).

are found not to be well bunched into Landau levels. Level repulsion leading to avoided crossings[6] is widely seen in the case $\sigma=0.5$ [Fig. 1(b)],[7] while true crossings between levels with different k values predominate in the case $\sigma=1$ [Fig. 1(a)].

The presence of many avoided crossing corresponds to chaos in the underlying classical dynamics. The latter was analyzed by the 2D bounce map for values of the arc length and skipping angle at successive bounces of an electron at the boundary.[5] For $\sigma\neq 1$, chaos around the unstable diametral orbit and/or flyaway chaos are found to dominate phase space, provided that the Larmor radius $r_c=mvc/eB$ satisfies $r_c/L\gtrsim\rho_{\min}$ for the smallest curvature radius $\rho_{\min}=\bar{b}^2/\bar{a}$. Noting $E=\frac{1}{2}mv^2$ for electron velocity v, we find $r_c/L=\bar{E}/\bar{B}^2$. Consistent with the classical findings, we clearly observe in Fig. 1(b) that avoided crossings dominate the spectra in the region $\bar{E}/\bar{B}^2\gtrsim 0.35$ for $\sigma=0.5$. More careful examination indicates that most of the avoided crossings in this region have much broader width than those discernible in the opposite region.

We consider a sample containing $2N$ electrons, and neglect the Zeeman splitting of the spin states. Then, in the free-electron ground state at a given value of the applied field, the lowest N levels $E_j(B)$ ($j=1,\ldots,N$) are filled with two electrons each, the Fermi level ϵ_F lying between $E_N(B)$ and $E_{N+1}(B)$. The isothermal susceptibility per electron at absolute zero is given by the second-order derivative (difference in our computations) of the total energy as[3,4]

$$\chi=-(2N)^{-1}\Delta^2\left[2\sum_{j=1}^{N}E_j\right]/\Delta B^2$$

$$=-\frac{2mL^2}{\hbar^2}\mu_B^2 N^{-1}\sum_{j=1}^{N}\frac{\Delta^2\bar{E}_j}{\Delta\bar{B}^2},\qquad(1)$$

where μ_B is the Bohr magneton. The factor 2 in the second expression denotes the spin degeneracy of each level. The contributions to the sum in Eq. (1) are computed separately for each manifold of different symmetry (parity for $\sigma\neq 1$, k value for $\sigma=1$). In this way, singularities of $\Delta^2\bar{E}_j/\Delta\bar{B}^2$ at true crossings are removed. $\Delta\bar{B}=5.0\times 10^{-2}$ is chosen here, which induces variations of eigenvalues $\{\bar{E}_j\}$ within their reliable decimal places. In Fig. 2, the negative of χ is shown as a function of $\bar{B}$ for the case of $N=100$ occupied levels, where approximately 50 levels are of even parity and the remaining ones are of odd parity.

For $\sigma=1$, χ is found to retain the essential features of

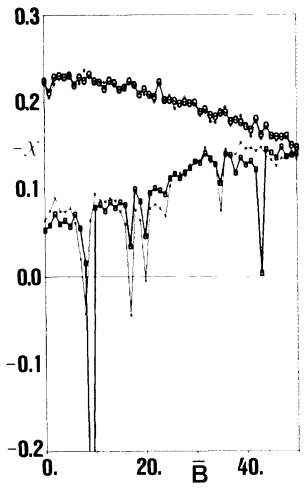

FIG. 2. Negative of diamagnetic susceptibility χ as a function of $\bar{B}$ for $N=100$. Circle and square symbols indicate $\sigma=1$ and 0.5 cases, respectively. Heavy symbols and lines denote combined contributions from both even- and odd-parity manifolds, while fine counterparts denote the contribution from the even-parity manifold alone with energies below ϵ_F. In Figs. 2 and 4, χ is scaled by $(2mL^2/\hbar^2)\mu_B^2$.

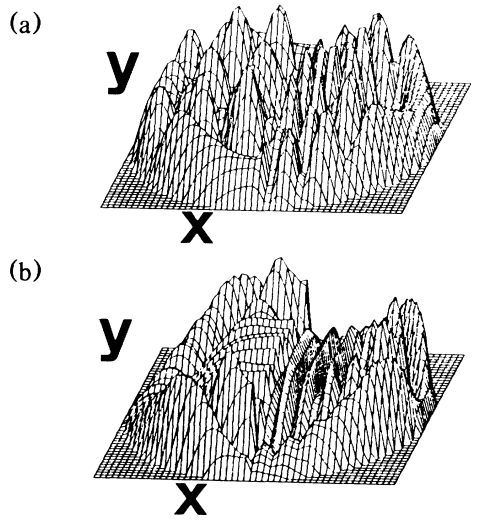

FIG. 3. Wavefunctions $|\Psi|$ at the avoided crossing indicated by arrow in Fig. 1(b). $\sigma=0.5$ and $\bar{B}=10$: (a) $\bar{E}_{32}=284.0230$; (b) $\bar{E}_{33}=285.1459$.

Landau diamagnetism in 2D systems: $-\chi$ takes the largest value in the vicinity of $\bar{B}=0$, and decreases monotonically with increasing B. Note that the value of χ determined by the contribution from the even-parity manifold alone exhibits almost identical results. Let us trace back to Fig. 1(a): All crossings appearing in this figure are true crossings between levels with different k. Therefore, each energy level shows a smooth variation with $\bar{B}$ with positive curvature $\Delta^2\bar{E}_j/\Delta\bar{B}^2>0$, which decreases with increasing B. The characteristics of the diamagnetic susceptibility for $\sigma=1$ shown in Fig. 1 are thus well explained by the regular behavior of the spectrum which is a direct consequence of the integrability of this case.

For $\sigma=0.5$, in contrast, χ shows remarkably different features: The value of $-\chi$ is greatly reduced at $\bar{B}=0$ as compared to the Landau value. It increases on the average with B, recovering the value for $\sigma=1$ only for $\bar{E}_{100}/\bar{B}^2\gtrsim\rho_{\min}$, i.e., for $\bar{B}\gtrsim 50$. This increase is accompanied by large fluctuations and anomalous dips (spikes), some of them even associated with positive values of χ. These features can be traced back to the behavior of the spectrum, which shows a multitude of avoided crossings (AC) in each of the two manifolds [see Fig. 1(b)]: The rapid variation of the two levels with $\bar{B}$ near an AC gives rise to anomalous contributions of $\Delta^2\bar{E}_j/\Delta\bar{B}^2$ of opposite signs. If the AC is narrow and lies below ϵ_F, the two contributions cancel in Eq. (1). But most AC's have widths of order of or greater than their mutual distance, such that their effects overlap. This leads to a rather flat variation of each level with $\bar{B}$, with a greatly reduced average curvature and large fluctuations due to the nonuniform distribution of AC's. With increasing B most AC's become extremely narrow, and the B dependence of the levels approaches that for $\sigma=1$. Anomalous dips in $-\chi$ occur for B values where ϵ_F lies within a gap of an AC. (From an experimental point of view, dips of this kind may be more or less suppressed by possible extrinsic disorder such as impurities.) Thus, the anomalous features of the diamagnetic susceptibility for $\sigma=0.5$ shown in Fig. 2 reflect the effects of level repulsion and avoided crossings typical for a nonintegrable system. Our additional data indicate an issue worth noting: The reduction of χ becomes more remarkable and its fluctuations become less pronounced with decreasing σ towards $\sigma=0$, while the opposite tendency is found with increasing σ towards $\sigma=1$.

Our findings cannot simply be interpreted in terms of the traditional concept of bulk states and edge states,[8] since such distinction of states is not possible for the case $r_c/L\sim 1$ considered in the present paper. Figure 3 shows an example of wave functions of a pair of states at a typical avoided crossing indicated in Fig. 1(b). They exhibit a complicated delocalized structure due to superposition of contributions from many k values. In fact, they can be attributed neither to bulk nor to edge states.

To examine the physical relevance of the characteristics in Fig. 2, we proceed to study the N dependence of χ for $\bar{B}=0$ and 25 in Figs. 4(a) and 4(b), respectively. There exists a clear tendency that differences of χ between $\sigma=1$ and 0.5 are maintained [Fig. 4(a)] or even enhanced [Fig. 4(b)] for increasing N as long as $\bar{E}_N/\bar{B}^2\gtrsim\rho_{\min}$ for the top of occupied levels in the system with $\sigma=0.5$. This ensures that our findings may be applied to thin conducting disks containing a low-density 2D electron gas. Let us consider, for example, the interface layer in semiconductor heterojunctions, where cur-

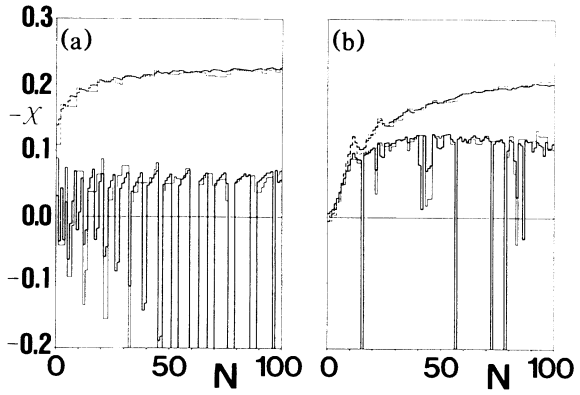

FIG. 4. $-\chi$ as a function of N ($1 \leqq N \leqq 100$): (a) $\bar{B}=0$; (b) $\bar{B}=25$. Broken and solid lines correspond to $\sigma=1$ and 0.5, respectively. The meaning of heavy and fine lines is the same as in Fig. 2.

rent works concentrate on the quantum Hall effect. In these systems, the electron concentration $\bar{n}$ is very low —typically, $\bar{n} \cong 10^{12}$ cm^{-2}. Noting that the Fermi wave number $k_F \cong n^{1/2}$ in 2D, we have $k_F \cong 10^6$ cm^{-1}. For the above $\bar{n}$, $N=10^2$ corresponds to $L \cong 10^{-5}$ cm. Then $\bar{E}_N \cong 8.0 \times 10^2$ for $\sigma=0.5$ and the interesting aspect of quantum chaos is seen for $0<\bar{B} \lesssim 50$, i.e., for $0<B \lesssim 2.5$ T. The de Broglie wavelength $\sim k_F^{-1}$ is large enough for the results to be insensitive to the lattice discreteness both within and along the boundary of the interface layer. In ordinary metal disks, on the other hand, $\bar{n}$ amounts to 10^{16} cm^{-1}, which corresponds to $k_F \cong 10^8$ cm^{-1}. Then the de Broglie wavelength is comparable to the lattice constant so that the results will be more or less modified. We should note one more comment regarding the experimental viability of our theoretical issue: Couplings of electrons with atomic-scale defects (e.g., impurities and imperfections) and with phonons at finite temperatures, which are inevitable in real materials, may yield additional avoided crossings in the electronic energy spectra. But they will occur in common in elliptic and circular billiards, resulting in a reduction of the common background for the diamagnetic susceptibility. So our predictions due to the deterministic chaos will still be verified in real experiments for small 2D devices so long as both the temperatures and the concentrations of atomic-scale defects are low enough.

In conclusion, chaotic dynamics in the nonintegrable elliptic billiard in a uniform magnetic field is found to induce a remarkable reduction and large fluctuations of the diamagnetic susceptibility, whereas the integrable circular billiard yields results close to Landau diamagnetism in 2D.

We have benefitted from discussions with the theory group at Institut für Physik der Universität Basel. One of us (K.N.) acknowledges valuable conversations with K. D. Schotte, H. J. Mikeska, H. Frahm, M. Nakayama, and S. A. Rice.

---

[a]On leave at the James Franck Institute, The University of Chicago, Chicago, IL 60637.

[1]See, e.g., *Chaotic Behavior in Quantum Mechanics,* edited by G. Casati (Plenum, New York, 1985); *Quantum Chaos and Statistical Nuclear Physics,* edited by T. H. Seligman and H. Nishioka (Springer-Verlag, Berlin, 1986). Strictly speaking, the terminology of "quantum chaos" has not yet been well defined at present. While the linear nature of Schrödinger equations leads to a suppression of chaotic diffusion of wave functions, quantum chaos in its reasonable sense may be conceivable in quantum many-body systems with infinite degrees of freedom and/or in some open quantum systems. Here we use this terminology for the quantum mechanics of systems whose classical version exhibits dynamical chaos, following most of the references above. A similar discussion is also given by M. Berry, in *Proceedings of the Royal Society Meeting on Dynamical Chaos, 4–5 February, 1987* (The Royal Society, London, 1987).

[2]N. Pomphrey, J. Phys. B **7**, 1909 (1974); D. W. Noid *et al.*, J. Chem. Phys. **78**, 4018 (1983); K. Nakamura *et al.*, Phys. Rev. Lett. **54**, 861 (1985). These papers propose as criteria of quantum chaos the second-order derivative of energy with respect to a nonintegrability parameter. On the other hand, some mathematical interrelations between the first- and second-order derivatives of energy are explored from a complete integrability viewpoint in K. Nakamura and M. Lakshmanan, Phys. Rev. Lett. **57**, 1661 (1986), and K. Nakamura and H. J. Mikeska, Phys. Rev. A **35**, 5294 (1987).

[3]R. Peierls, Z. Phys. **80**, 763 (1933), and **81**, 186 (1933). See also N. W. Ashcroft and N. D. Mermin, *Solid State Physics* (Cornell Univ. Press, Ithaca, NY, 1976). While extensive studies on the 2D version of the metallic diamagnetism have been made [e.g., R. S. Markiewicz *et al.*, Phys. Rev. B **36**, 7859 (1987); L. Wang and R. F. O'Connell, Phys. Rev. B **37**, 3052 (1988)], most of them are confined to the case in which Landau levels, broadened or not, play a fundamental role. In the present text, our main concern lies in mesoscopic systems with their linear dimension smaller than the inelastic scattering length of electrons, because our theoretical issue will be based on the deterministic chaos. To our knowledge, no clear experiment of the low-field diamagnetic susceptibility seems to have been performed on small 2D systems which satisfy the above condition.

[4]R. Peierls, *Surprises in Theoretical Physics* (Princeton Univ. Press, Princeton, 1979).

[5]M. Robnik and M. V. Berry, J. Phys. A **18**, 1361 (1985); M. Robnik, in *Nonlinear Phenomena and Chaos,* edited by S. Sarker (Hilger, Bristol, 1986).

[6]J. von Neumann and E. P. Wigner, Z. Phys. **30**, 467 (1929).

[7]Some of the local aspect, e.g., the GOE-type level-spacing distribution, was pointed out by O. Bohigas *et al.* in *Quantum Chaos and Statistical Nuclear Physics,* edited by T. H. Seligman and H. Nishioka (Springer-Verlag, Berlin, 1986).

[8]E. Teller, Z. Phys. **67**, 311 (1931).

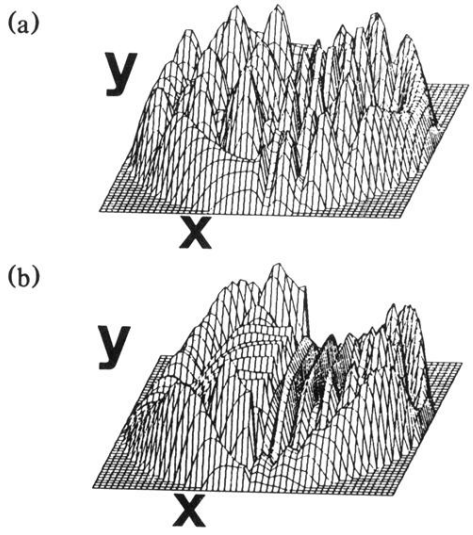

FIG. 3. Wavefunctions $|\Psi|$ at the avoided crossing indicated by arrow in Fig. 1(b). $\sigma=0.5$ and $\bar{B}=10$: (a) $\bar{E}_{32}=284.0230$; (b) $\bar{E}_{33}=285.1459$.